Journal of Physics and Chemistry of Solids 69 (2008) 3191–3194

Contents lists available at ScienceDirect

Journal of Physics and Chemistry of Solids

journal homepage: www.elsevier.com/locate/jpcs

Anisotropic scattering and superconductivity in high-T_c cuprates

M.M.J. French [a], M. Abdel-Jawad [a], J.G. Analytis [a], L. Balicas [b], N.E. Hussey [a,*]

[a] H.H. Wills Physics Laboratory, University of Bristol, Bristol BS8 1TL, UK
[b] National High Magnetic Field Laboratory, Florida State University, Tallahassee, FL 32306, USA

ARTICLE INFO

PACS:
74.72.Jt
75.47.−m

Keywords:
A. Superconductors
D. Electrical conductivity
D. Fermi surface
D. Transport properties
D. Superconductivity

ABSTRACT

The isotropic and anisotropic components of the transport scattering rate in overdoped $Tl_2Ba_2CuO_{6+\delta}$ are determined for a range of T_c values between 15 and 35 K by angle-dependent magnetoresistance measurements at $T = 40$ K. The anisotropic scattering term is found to scale linearly with T_c and appears to vanish at the point where superconductivity is destroyed, establishing a clear link between the superconducting and normal state physics. Comparison with results from angle resolved photoemission spectroscopy suggests that the transport and quasi-particle lifetimes are very different.

1. Introduction

Normal state transport properties of superconductors frequently serve as a useful guide to the nature of the electron pairing mechanism. In conventional superconductors, for example, the strength of the electron–phonon (e–ph) coupling is manifested in the magnitude of the normal state resistivity, or more specifically, the strength of the transport scattering rate $1/\tau_{tr}$. At elevated temperatures, where the resistivity is T-linear, $1/\tau_{tr}$ is related to the e–ph coupling constant λ_{e-ph} via $\hbar/\tau_{tr} = 2\pi k_B T_c \lambda_{e-ph}$ where T_c is the superconducting transition temperature.

In high temperature superconductors (HTSC), the doping dependence of the in-plane resistivity $\rho_{ab}(T)$ is largely generic and appears tied to the T_c parabola (for a review see [1]), suggesting an intimate relation between the normal state scattering and superconductivity. At optimal doping, for example, ρ_{ab} is strictly T-linear [2] over a wide temperature range [3] whilst the Hall coefficient R_H has its strongest T-dependence [4]. Despite intense efforts, however, any direct correlation between superconductivity and $1/\tau_{tr}$ has failed to materialize, largely due to difficulties in establishing the intrinsic T- and momentum-dependence of $1/\tau_{tr}$ itself.

Progress on this front was made recently through developments in the analysis of angle-dependent magnetoresistance (ADMR) measurements on HTSC [5–7]. ADMR measurements, angular variations in the interlayer resistivity $\rho_\perp$ at constant temperature T and magnetic field H [8], have provided detailed information of the Fermi surface (FS) in a variety of layered metals [9–11]. By incorporating basal-plane anisotropy into the ADMR analysis, new information, namely the T- and momentum ($\mathbf{k}$-) dependence of the scattering rate $\Gamma(T,\mathbf{k})$ could be extracted. Subsequent ADMR measurements on heavily overdoped (OD) $Tl_2Ba_2CuO_{6+\delta}$ (Tl2201) revealed that $\Gamma(T,\mathbf{k})$ consisted of two components, one isotropic and quadratic in T, the other anisotropic, maximal near the saddle points at (π, 0) and proportional to T [5]. Significantly, the deduced scattering rate could account for both $\rho_{ab}(T)$ and $R_H(T)$ in this compound.

In this report, ADMR measurements at $T = 40$ K and $\mu_0 H = 45$ T are compared for a number of OD Tl2201 crystals with differing T_c values between 15 and 35 K. The strength of the anisotropic scattering is found to scale linearly with T_c, *extrapolating to zero at the doping level where superconductivity vanishes*. This new correlation implies that it is the *anisotropic* scattering mechanism that is intimately related to the mechanism of HTSC. In marked contrast to what has been inferred for the quasi-particle lifetime from angle resolved photoemission spectroscopy (ARPES) [12,13], no sign reversal of the anisotropy is observed. Finally, our results shed new light on the doping evolution of both $\rho_{ab}(T)$ and $R_H(T)$ in OD cuprates.

2. Experimental method and results

A total of six self-flux grown crystals [14] (typical dimensions $0.3 \times 0.3 \times 0.03\,mm^3$) were annealed at temperatures $300\,^\circ C \leqslant T \leqslant 600\,^\circ C$ in flowing O_2 and mounted in a c-axis quasi-Montgomery configuration. ADMR were measured on a two-axis

* Corresponding author. Tel.: +44 1179288140.
E-mail address: n.e.hussey@bristol.ac.uk (N.E. Hussey).

0022-3697/$ - see front matter Crown Copyright © 2008 Published by Elsevier Ltd. All rights reserved.
doi:10.1016/j.jpcs.2008.06.070

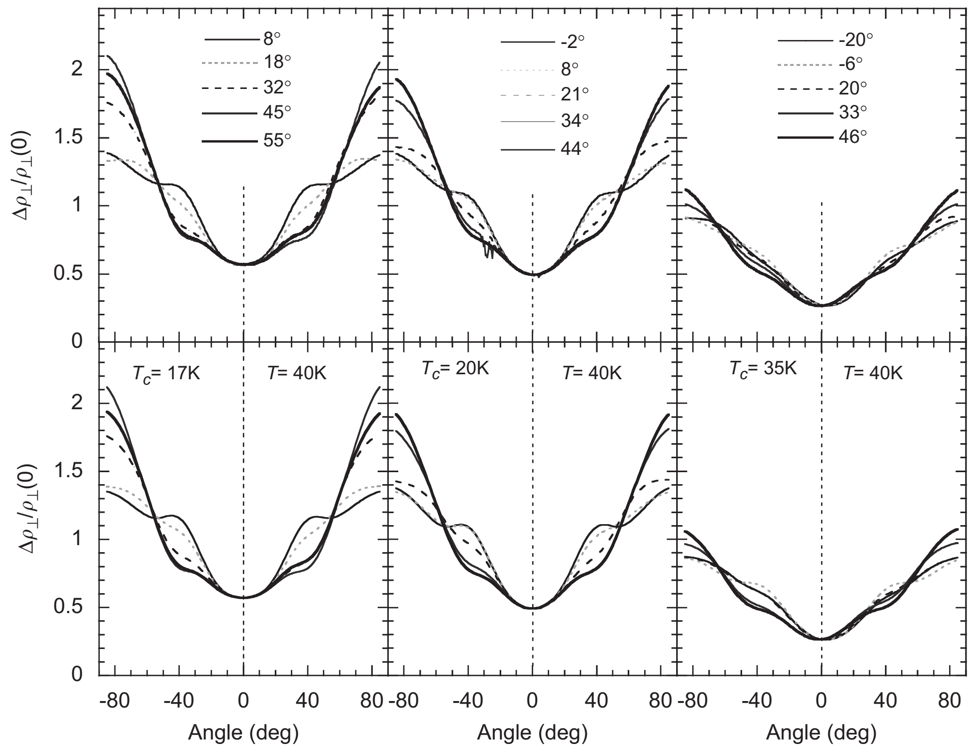

Fig. 1. Top panels: angle-dependent magnetoresistance sweeps for three different samples of overdoped Tl2201 with T_c of 17 K (Tl17K—left panel), 20 K (Tl20K—middle panel) and 35 K (Tl35K—right side) measured at 40 K and 45 T. Bottom panels: the least-square fits to each data set, respectively. The asymmetry around $\theta = 0$ arises from slight misalignment of the crystalline c-axis with respect to the rotational platform. The inclusion of a coordinate axis rotated with respect to the platform axis can account for such a distortion and has been added to our fitting routine. This correction, however, has a negligible effect on the parameters obtained.

rotator in the 45 T hybrid magnet at the NHMFL in Florida using a conventional four-probe ac lock-in technique. The orientation of the crystal faces was indexed for a number of crystals using a single crystal X-ray diffractometer.

The top panels of Fig. 1 show polar ADMR data $\Delta\rho_\perp/\rho_\perp(0)$ (normalized to their zero-field value) at different azimuthal angles ϕ (relative to the Cu–O–Cu bond direction) for three crystals Tl17K, Tl20K and Tl35K (the numbers relate to their T_c values). Similar data for the other three crystals measured in this study (Tl15Ka, Tl15Kb and Tl32K) have already been published elsewhere [5,15]. Note that $\Delta\rho_\perp/\rho_\perp(0)$ is significantly larger for the lower T_c crystals. Moreover, near $\mathbf{H}\|c$ ($\theta = 0$), the Tl35K curves are more V-shaped than rounded. As shown below, these features are caused by the higher T_c, less OD samples possessing a significantly larger relative basal-plane anisotropy in $\omega_c\tau$, the product of the cyclotron frequency and the transport lifetime [5].

In order to extract information on the FS and $\omega_c\tau$, we carried out a least-square fitting of the data using the Shockley–Chambers tube integral form of the Boltzmann transport equation modified for a quasi-2D metal with a four-fold anisotropic scattering rate $1/\tau(\varphi) = (1 + \alpha\cos 4\varphi)/\tau^0$ and anisotropic in-plane velocity $v_F(\varphi)$, incorporated via $1/\omega_c(\varphi) = (1 + \beta\cos 4\varphi)/\omega_c^0$ [5,6]. The sign of α defines the azimuthal location of maximal scattering. The FS wavevector $k_F(\theta,\varphi)$ was parameterized into lowest order harmonic components satisfying the body-centered tetragonal symmetry of Tl2201 [16]:

$$\begin{aligned} k_F(\theta,\varphi) = k_{00} - k_{40}\cos 4\varphi - k_{21}\cos(k_z c/2)\sin 2\varphi \\ - k_{61}\cos(k_z c/2)\sin 6\varphi \\ - k_{101}\cos(k_z c/2)\sin 10\varphi \end{aligned} \tag{1}$$

where k_z is the c-axis wavevector and c is the interlayer spacing. Note that k_{21}, k_{61} and k_{101} are small compared to k_{00}, the radius of the cylindrical FS (about the zone corners), and k_{40}, its in-plane squareness, and only their ratio (e.g. k_{61}/k_{21}) can be determined to good accuracy. To minimize the number of free parameters, we fix $k_{101}/k_{21} = k_{61}/k_{21} - 1$ such that $t_\perp(\varphi)$ vanishes at both the nodes and the anti-nodes [11,17] and fix k_{00} using the empirical relation $T_c/T_c^{\max} = 1 - 82.6(p - 0.16)^2$ with $T_c^{\max} = 92\,\mathrm{K}$ and $(\pi k_{00}^2)/(2\pi/a)^2 = (1+p)/2$ [18]. The coefficient β depends largely on our choice of k_{61}/k_{21} with the best least-square (χ^2) values giving $\beta = 0 \pm 0.1$ for $0.6 \leqslant k_{61}/k_{21} \leqslant 0.8$ for all samples. The sum $\alpha + \beta$ was much less sensitive to variations in k_{61}/k_{21}, however, and for simplicity, we assume hereafter $\omega_c(\varphi) = \omega_c^0$.

The best fits, shown in the bottom panels of Fig. 1, are all excellent and the four remaining fitting parameters (see Ref. [15]) are well constrained due to the wide range of polar and azimuthal angles studied. Within our experimental resolution, the FS parameters appear to have negligible doping dependence. Moreover, the projected in-plane FS is found to be in good agreement with recent ARPES measurements on the same compound [13]. The anisotropy parameter α increases with rising T_c whilst $\omega_c^0\tau^0$ shows the opposite trend (as is evident from the overall reduction in the ADMR signal in Fig. 1).

3. Discussion and analysis

Our previous T-dependent analysis of Tl15Ka implied the presence of two inelastic scattering channels in the current response of OD Tl2201 [5]. Accordingly we split $1/\omega_c^0\tau(\varphi)$ into isotropic and anisotropic components $\gamma_{\mathrm{iso}} = (1-\alpha)/\omega_c^0\tau^0$ and $\gamma_{\mathrm{aniso}} = 2\alpha/\omega_c^0\tau^0\cos^2 2\varphi$. In Tl15Ka, $\gamma_{\mathrm{iso}} \sim A + BT^2$, reflecting a combination of impurity and electron–electron scattering, whilst $\gamma_{\mathrm{aniso}} \sim CT$ [5], the microscopic origin of which has yet to be identified. The doping (T_c) dependence of γ_{iso} and γ_{aniso}